PROCEEDINGS OF SCIENCE

Geant4 simulations of the influence of contamination and roughness of the detector surface on background spectra in CRESST

C. Grüner,[b,c,*] **G. Angloher,**[a] **S. Banik,**[b,c] **G. Benato,**[d] **A. Bento,**[a,i] **A. Bertolini,**[a] **R. Breier,**[e] **C. Bucci,**[d] **J. Burkhart,**[b] **L. Canonica,**[a,m] **A. D'Addabbo,**[d] **S. Di Lorenzo,**[a] **L. Einfalt,**[b,c] **A. Erb,**[f,j] **F. v. Feilitzsch,**[f] **S. Fichtinger,**[b] **D. Fuchs,**[a] **A. Garai,**[a] **V.M. Ghete,**[b] **P. Gorla,**[d] **P.V. Guillaumon,**[d] **S. Gupta,**[b] **D. Hauff,**[a] **M. Ješkovský,**[e] **J. Jochum,**[g] **M. Kaznacheeva,**[f] **A. Kinast,**[f] **H. Kluck,**[b] **H. Kraus,**[h] **S. Kuckuk,**[g] **A. Langenkämper,**[a] **M. Mancuso,**[a] **L. Marini,**[d,k] **B. Mauri,**[a] **L. Meyer,**[g] **V. Mokina,**[b] **M. Olmi,**[d] **T. Ortmann,**[f] **C. Pagliarone,**[d,l] **L. Pattavina,**[d,f] **F. Petricca,**[a] **W. Potzel,**[f] **P. Povinec,**[e] **F. Pröbst,**[a] **F. Pucci,**[a] **F. Reindl,**[b,c] **J. Rothe,**[f] **K. Schäffner,**[a] **J. Schieck,**[b,c] **S. Schönert,**[f] **C. Schwertner,**[b,c] **M. Stahlberg,**[a] **L. Stodolsky,**[a] **C. Strandhagen,**[g] **R. Strauss,**[f] **I. Usherov,**[g] **F. Wagner,**[b] **M. Willers**[f] **and V. Zema**[a] **(CRESST collaboration)**

[a] *Max-Planck-Institut für Physik, D-80805 München, Germany*
[b] *Institut für Hochenergiephysik der Österreichischen Akademie der Wissenschaften, A-1050 Wien, Austria*
[c] *Atominstitut, Technische Universität Wien, A-1020 Wien, Austria*
[d] *INFN, Laboratori Nazionali del Gran Sasso, I-67100 Assergi, Italy*
[e] *Comenius University, Faculty of Mathematics, Physics and Informatics, 84248 Bratislava, Slovakia*
[f] *Physik-Department, Technische Universität München, D-85747 Garching, Germany*
[g] *Eberhard-Karls-Universität Tübingen, D-72076 Tübingen, Germany*
[h] *Department of Physics, University of Oxford, Oxford OX1 3RH, United Kingdom*
[i] *also at: LIBPhys-UC, Departamento de Fisica, Universidade de Coimbra, P3004 516 Coimbra, Portugal*
[j] *also at: Walther-Meißner-Institut für Tieftemperaturforschung, D-85748 Garching, Germany*
[k] *also at: GSSI-Gran Sasso Science Institute, I-67100 L'Aquila, Italy*
[l] *also at: Dipartimento di Ingegneria Civile e Meccanica, Universitá degli Studi di Cassino e del Lazio Meridionale, I-03043 Cassino, Italy*
[m] *present address: INFN, Sezione di Milano LASA, I-20054 Segrate, Milano, Italy*

E-mail: christoph.gruener@oeaw.ac.at

[*] Speaker

PoS(TAUP2023)092

CRESST is an experiment for the direct detection of dark matter, capable of detecting nuclear recoils down to 10 eV, which results in an impressive sensitivity for sub-GeV dark matter particles. For a better understanding of the measured background a background model is developed. The background components are considered via Geant4 simulations. At the current state, the CRESST background model only considers bulk contaminations and treats all detector surfaces as perfect plains.

This contribution presents potential effects of a surface contamination with radiogenic nuclides, in combination with the influence of the crystals surface roughness. Nuclide decays near the crystal surface may lead to partial energy deposition inside the detector, potentially causing MeV energy events to influence the background in the keV energy range. Since default Geant4 is not capable of simulating a rough surface, a new extension for simulating a rough surface is developed and the impact of different roughness configurations is studied.

XVIII International Conference on Topics in Astroparticle and Underground Physics (TAUP2023)
28.08_01.09.2023
University of Vienna

1. Introduction

CRESST is a direct detection dark matter experiment, probing the parameter space for low mass ($\lesssim$ 1 GeV/c^2) WIMPs with cryogenic crystals (~15 mK). Different types of materials are used [1–3], e.g. $CaWO_4$ [1]. To protect the experiment against atmospheric background, it is located ~1400 m below the Gran Sasso massif at Laboratori Nazionali del Gran Sasso (LNGS) and is equipped also with further shieldings and a muon veto [4]. An electromagnetic background model using bulk contaminations was developed to study the residual background with Monte Carlo simulations [4]. Spectral templates representing the distribution of energy depositions expected from different backgrounds are simulated. The simulation is done with ImpCRESST, a Geant4-based simulation tool developed and used by CRESST [4]. Afterwards, the templates are fitted to experimental background data using a newly developed likelihood normalisation method [5], see Fig. 1 for the energy range dominated by α-decays. With this method the experimental data can be covered[1] up to

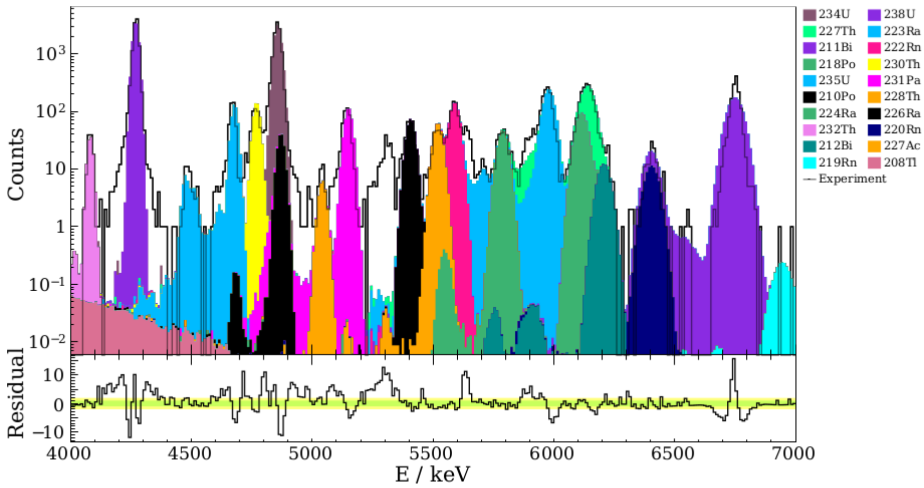

Figure 1: Simulated spectra caused by α-decaying bulk-contaminants (colored, filled histrograms) fitted [4, 5] to experimental high energy data (black, open histogram) of CRESST's TUM40 detector [6]. An interactive version of this plot is available [5].

99.6 % [5]. But some features could not be explained by the simulation, see Fig. 1. The remaining, uncovered parts are, among others, tails around the ^{238}U, ^{234}U or ^{231}Pa peak or a single peak at an energy of ~5300 keV. This is a hint for either: missing contaminants or it may be an effect of surface contamination and surface roughness, which is not yet included in CRESST's background model. Near surface decays can lead to decay products leaving the detector, depositing only a share of their decay-energy. For example, air-borne ^{222}Rn may contaminate the crystal surface during the detector production; subsequent decays would cause surface contaminations with ^{210}Po, observed by CRESST [7], and ^{210}Pb, observed by CUORE [8].

This study investigates the effect of decaying contaminants in the vicinity of the crystals surface on CRESST's background spectrum. First, I will show different types of surface roughness profiles of crystals (Section 2). Then two surface contamination models are presented (Section 3) and different simulated energy deposition spectra generated by using these models are discussed

[1] Coverage is defined as the ratio of expected events over the measured number of events in the experiment

(Section 4). At last the impact of different surface contaminations on CRESST's background model is investigated (Section 5). We conclude in Section 6.

2. Surface Roughness of $CaWO_4$ Crystals

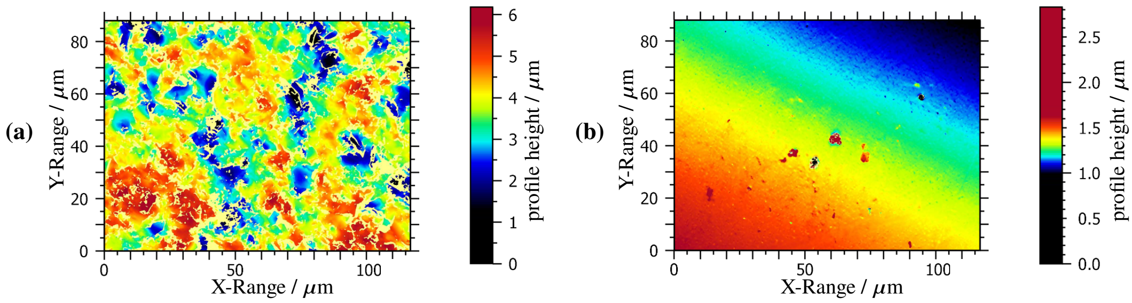

Figure 2: Surface roughness profiles of a diffused (a) and polished (b) $CaWO_4$ crystal, TUM73 and TUM84 respectively. The surfaces were examined by V. Mokina, using a LEICA DCM8 microscope.

The focus of this work is an extension of the ImpCRESST code that enables the inclusion of surface background components in CRESST's background model. As example we will apply it to highly radiopure $CaWO_4$ crystals which were grown at TU Munich as target material for detector modules [1]. To consider the impact of different surface treatments on the results, we study diffused and polished $CaWO_4$ crystals; their surface roughness profiles were examined by V. Mokina, using a LEICA DCM8 microscope, see Fig. 2. Later we will compare our results to the TUM40 detector [6], which had also a diffused surface like TUM73.

3. Modeling of Surface Contaminations

To simulate surface contaminations with ImpCRESST, two different particle generators were developed and studied:

Method A, developed by A. Rabensteiner, places contamination nuclei in the vicinity below the plain surface of a given volume. The placement depth x of the contaminants below the surface can be sampled from different distributions: an exponential $P(x;\lambda) \propto \exp(x/\lambda)$, a normal $N(x;\mu,\sigma)$ and a delta distribution $P(x;x_0) = \delta(x-x_0)$. CUORE's simulation [8] is comparable to this method.

Method B generates the contamination of a "realistic rough" surface using two newly developed, user controlled Geant4 modules: 1) *surface generator*, and 2) *particle generator*.

1) creates a patch of spikes (up to 1000 x 1000) which can vary in height, width and number of spikes. 2) places nuclides exactly at the surface of the generated spikes. Details like the available spike shapes are given in the appendix.

4. Simulation of Background from Surface ^{210}Po

To study contaminants on a flat surface we apply method A. Fig. 3 shows the simulated energy deposition of 5e4 ^{210}Po nuclide decays in the vicinity of the flat surface; their placement depth follows either a delta (Fig. 3a) or an exponential distribution (Fig. 3b). From Fig. 3a one can see the principal impact of the placement depth of ^{210}Po nuclei on the spectrum of energy deposition.

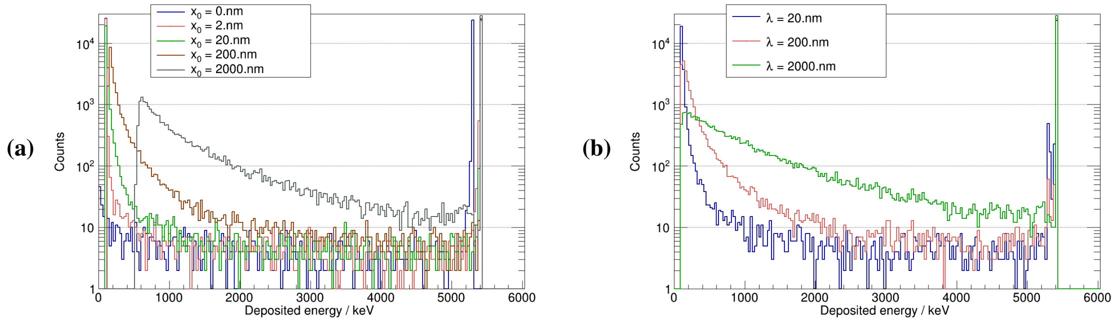

Figure 3: Simulated energy deposition caused by 5e4 decaying ^{210}Po nuclei placed in the vicinity of the surface of a simulated $CaWO_4$ crystal. The placement depth x of nuclei is following a distribution function depending on the distance to the surface: (a) a delta distribution $\delta(x - x_0)$, (b) an exponential distribution $\exp(x/\lambda)$.

Three peaks are visible: a peak at 103 keV when only the recoiling ^{206}Pb nucleus is absorbed, a peak at 5304 keV when only the α is absorbed, and a mixed ^{206}Pb+α peak at 5407 keV when both are absorbed. With increasing depth the pure α and ^{206}Pb peak intensity decrease and the mixed peak intensity increases as it is more likely that both are at least partially absorbed when they are placed farther away from the surface. For the same reasons, the remaining ^{206}Pb recoil peak is shifted to higher energies and broadens. The shift depends on the energy α-particles deposit while escaping the detector while the whole energy of ^{206}Pb is absorbed by the crystal. The increase of counts in the medium energy range between the ^{206}Pb and α peak can be explained by the same effect.

Fig. 3b shows the energy deposition for an exponential distributed placement depth. Even in this more realistic scenario, all three aforementioned peaks are visible. However, with increasing parameter λ the ^{206}Pb peak does not get shifted as in Fig. 3a. This is because even for large values of λ, some nuclei always decay in the vicinity of the surface and the α-particle can escape without depositing energy in the detector. To study the effects of surface roughness we apply method B.

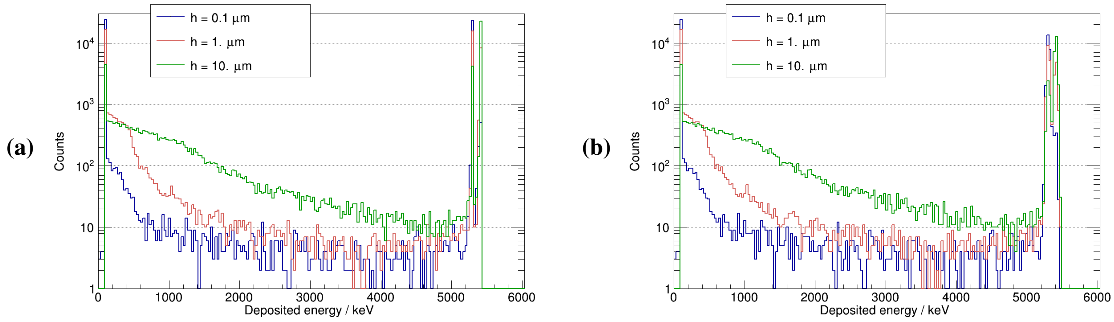

Figure 4: Simulated energy deposition of 5e4 decaying ^{210}Po nuclei placed exactly at the boundary of a rough surface of a $CaWO_4$ crystal without energy resolution (a) and with applied energy resolution (b). The roughness is modelled by spikes of 2 µm width and height h.

Again, we simulated 5e4 decays of ^{210}Po, but this time the nuclei are placed exactly at the boundary of a simulated rough detector surface. The aforementioned ^{206}Pb, α and ^{206}Pb+α peaks are visible and the overall shape of the energy deposition spectrum looks the same as for the flat surface

(Fig. 3). However, differences are visible: In Fig. 4a the ^{206}Pb peak has a non-smooth tail towards higher energies. This is due to the placement of ^{210}Po nuclides exactly at the surface which allows α-particles to escape without passing through any detector volume. The medium energy range shows a flattening towards the ^{206}Pb peak. With increasing spike height the α peak decreases and the ^{206}Pb+α peak increases. This is because of the increasing probability that both, the α-particle and the ^{206}Pb nuclide hit the detector volume after the decay of ^{210}Po. In Fig. 4b time and energy resolution of the TUM40 detector [4] is applied to the simulation data. The overall spectrum does not change except for the smearing of the α and the ^{206}Pb+α peak.

5. Impact of Surface Contaminations on CRESST's Background Model

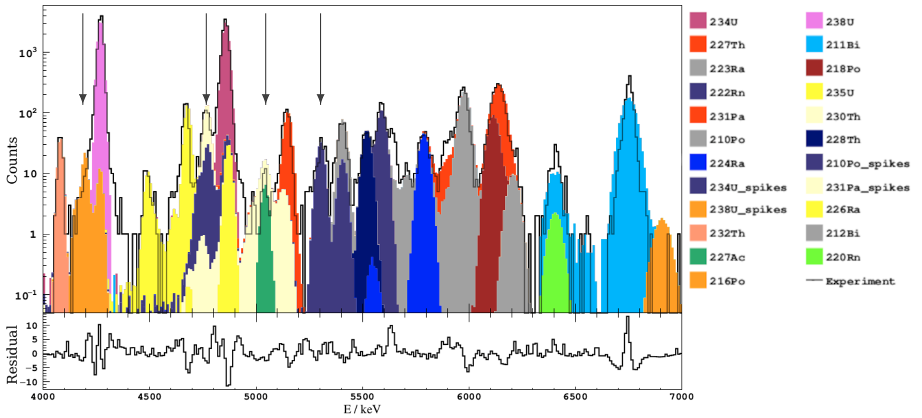

Figure 5: Simulated spectra caused by α-decaying bulk- and surface-contaminants (colored, filled histograms) fitted [4, 5] to experimental data (black, open histogram) of CRESST's TUM40 detector [6]. The surface contaminants ^{210}Po, ^{231}Pa, ^{234}U and ^{238}U are placed on a rough, spiked surface, following method B of this paper, and are marked with the suffix "spikes".

Using the new method B, templates for surface contaminations by ^{210}Po, ^{231}Pa, ^{234}U and ^{238}U are generated and fitted to TUM40 high energy data using the likelihood normalisation method [5], see Fig. 5. Compared to the bulk-only simulation (Fig. 1) it can be seen that these added surface templates can fill so-far unaccounted gaps: the peak at ~5300 keV is caused by surface ^{210}Po, the left tail of the bulk ^{238}U peak is filled by surface ^{238}U and the left tail of the bulk ^{231}Pa peak is filled by surface ^{231}Pa.

6. Conclusion

We simulated for the first time the potential contribution of near surface contaminations to CRESST's background budget. We have studied two different methods for simulating surface contaminations on the example of ^{210}Po (Section 4): method A distributes contaminants in the vicinity of an actual flat surface modelling a polished crystal surface, method B places contaminants on a rough surface modelling a diffused surface. The energy deposition spectra simulated using these methods show a similar general behaviour, but differ below 2 MeV.

We showed (Section 5) that surface contamination with ^{210}Po, ^{231}Pa, ^{234}U and ^{238}U on a rough surface (simulated with method B) can explain background observed with CRESST's TUM40

PoS(TAUP2023)092

detector, which could not yet be attributed with CRESST's bulk-only background model. Hence, this work is an important first step for the full consideration of surface backgrounds in our background model.

7. Acknowledgments

This work has been funded by the Deutsche Forschungsgemeinschaft (DFG, German Research Foundation) under Germany's Excellence Strategy – EXC 2094 – 390783311 and through the Sonderforschungsbereich (Collaborative Research Center) SFB1258 'Neutrinos and Dark Matter in Astro- and Particle Physics', by the BMBF 05A20WO1 and 05A20VTA and by the Austrian science fund (FWF): I 5420-N. FW was supported through the Austrian research promotion agency (FFG), project ML4CPD. SG was supported through the FWF project STRONG-DM (FG1). JB and HK were funded through the FWF project P 34778-N ELOISE. The Bratislava group acknowledges a partial support provided by the Slovak Research and Development Agency (projects APVV-15-0576 and APVV-21-0377). The computational results presented were partially obtained using the CLIP cluster and the Max Planck Computing and Data Facility (MPCDF).

References

[1] A. Münster, *High-Purity $CaWO_4$ Single Crystals for Direct Dark Matter Search with the CRESST Experiment*, Ph.D. thesis, TU München, 2017.

[2] G. Angloher, G. Benato, A. Bento, E. Bertoldo, A. Bertolini, R. Breier et al., *Probing spin-dependent dark matter interactions with ^{6}Li*, The European Physical Journal C **82** (2022) .

[3] G. Angloher, S. Banik, G. Benato, A. Bento, A. Bertolini, R. Breier et al., *Results on sub-GeV dark matter from a 10 eV threshold CRESST-III silicon detector*, Physical Review D **107** (2023) .

[4] A.H. Abdelhameed, G. Angloher, P. Bauer, A. Bento, E. Bertoldo, R. Breier et al., *Geant4-based electromagnetic background model for the CRESST dark matter experiment*, The European Physical Journal C **79** (2019) .

[5] G. Angloher, S. Banik, G. Benato, A. Bento, A. Bertolini, R. Breier et al., *High-Dimensional Bayesian Likelihood Normalisation for CRESST's Background Model*, 2307.12991.

[6] A. Erb and J.-C. Lanfranchi, *Growth of high-purity scintillating $CaWO_4$ single crystals for the low-temperature direct dark matter search experiments CRESST-II and EURECA*, CrystEngComm **15** (2013) 231.

[7] A. Kinast, *Enhancing the Dark Matter Sensitivity of CRESST: Purification, Stress Reduction and 17O Enrichment of $CaWO_4$ Target Crystals*, Ph.D. thesis, TU München, 2023.

[8] C. Alduino, K. Alfonso, D.R. Artusa, F.T. Avignone, O. Azzolini, T.I. Banks et al., *The projected background for the CUORE experiment*, The European Physical Journal C **77** (2017) .

Appendix

The repetitive placement of multiple but uniform spikes (Fig. 6) next to each other is representing a rough surface (Fig. 7).

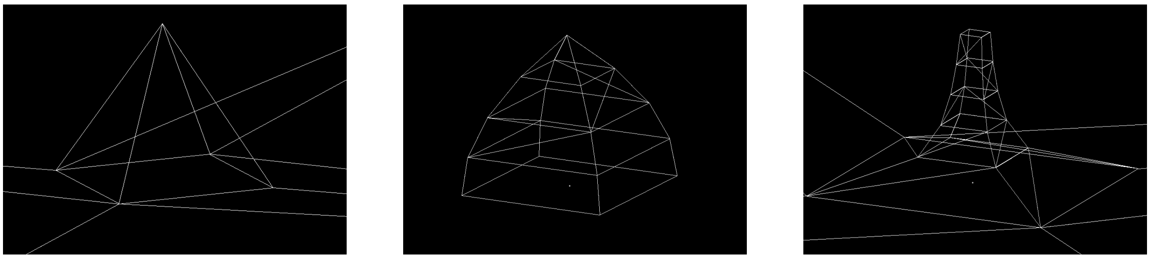

(a) **(b)** **(c)**

Figure 6: Visualization of different implementations of simulated spikes in Geant4: (a) simplest form of a spike, basis is a Geant4 tetrahedron. (b) multiple layers of Geant4 tetrahedrons form the spike, the outer surface approximates a squared function. (c) multiple layers of Geant4 tetrahedrons form the spike, the outer surface approximates $1/x$.

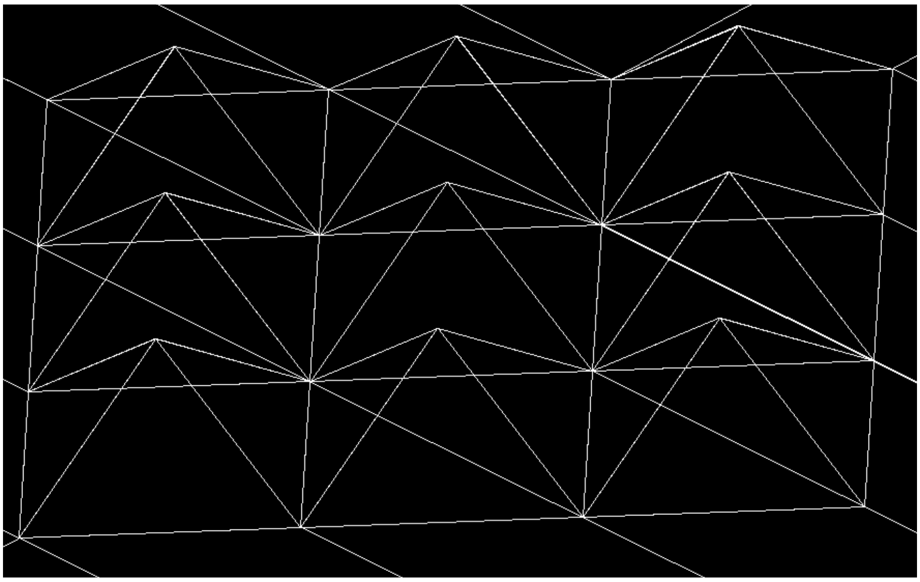

Figure 7: Geant4 visualization of 3x3 spikes placed at the surface of a target volume to simulate a patch of rough surface.